Rational design of shepherdin, a novel anticancer agent

Janet Plescia,[1] Whitney Salz,[1] Fang Xia,[1] Marzia Pennati,[2] Nadia Zaffaroni,[2] Maria Grazia Daidone,[2] Massimiliano Meli,[2,3] Takehiko Dohi,[1] Paola Fortugno,[1] Yulia Nefedova,[4] Dmitry I. Gabrilovich,[4] Giorgio Colombo,[3] and Dario C. Altieri[1,*]

[1]Department of Cancer Biology and the Cancer Center, University of Massachusetts Medical School, Worcester, Massachusetts 01605
[2]Dipartimento di Oncologia Sperimentale, Istituto Nazionale per lo Studio e la Cura dei Tumori, 20133 Milano, Italy
[3]Istituto di Chimica del Riconoscimento Molecolare, 20131 Milano, Italy
[4]Moffitt Cancer Center, University of South Florida, Tampa, Florida 33612
*Correspondence: dario.altieri@umassmed.edu

Summary

Anticancer agents that selectively kill tumor cells and spare normal tissues are urgently needed. Here, we engineered a cell-permeable peptidomimetic, shepherdin, modeled on the binding interface between the molecular chaperone Hsp90 and the antiapoptotic and mitotic regulator, survivin. Shepherdin makes extensive contacts with the ATP pocket of Hsp90, destabilizes its client proteins, and induces massive death of tumor cells by apoptotic and nonapoptotic mechanisms. Conversely, shepherdin does not reduce the viability of normal cells, and does not affect colony formation of purified hematopoietic progenitors. Systemic administration of shepherdin in vivo is well tolerated, and inhibits human tumor growth in mice without toxicity. Shepherdin could provide a potent and selective anticancer agent in humans.

Introduction

Despite a better understanding of the biology of tumor cells (Vogelstein and Kinzler, 2004), the treatment of most cancers has not significantly changed for the past three decades, and drugs that do not discriminate between tumor cells and normal tissues remain mainstays of anticancer therapy. Disabling an essential oncogenic pathway has produced encouraging results in the management of certain malignancies (O'Dwyer and Druker, 2000; Paez et al., 2004). However, this type of "targeted" therapy may not be immediately applicable to most solid tumors, in which the accumulation of numerous molecular abnormalities (Vogelstein and Kinzler, 2004) and genomic instability (Sieber et al., 2003) may elude the identification of a single, driving oncogene. Conversely, pathways that intersect multiple essential functions of tumor cells may provide broader therapeutic prospects. A candidate for such an approach is survivin, an essential regulator of cell proliferation, differentiation, and apoptosis that is sharply overexpressed in cancer versus normal tissues, and frequently linked to unfavorable disease outcome (Altieri, 2003). Because of its role at a crossroad of multiple cellular functions (Okada and Mak, 2004), and the likelihood that survivin antagonists may have selective antitumor efficacy in vivo (Altieri, 2003), drug discovery efforts to target the survivin pathway in cancer are being vigorously pursued, and clinical testing of survivin antisense oligonucleotides has recently begun. A nodal point for the multiple functions of survivin in tumor cells is its association with heat shock protein 90 (Hsp90), which is required to preserve survivin stability, in vivo (Fortugno et al., 2003). Hsp90 is an ATPase-directed molecular chaperone that oversees protein folding quality control during the cellular stress response, and whose repertoire of client proteins is typically restricted to signaling molecules involved in cell proliferation and cell survival (Young et al., 2001). This is thought to play a key role in cancer, where Hsp90 is commonly upregulated, and its stress response recognition may help promote tumor cell adaptation in face of unfavorable environments (Isaacs et al., 2003). Conversely, this pathway has created a viable therapeutic opportunity (Sausville et al., 2003), and molecular targeting of Hsp90 ATPase activity by the class of ansamycin antibiotics prototypically exemplified by Geldanamycin (GA) (Neckers and Ivy, 2003) has shown promising anticancer activity for disabling multiple signaling networks required for tumor cell maintenance (Basso et al., 2002).

Here, we used structure-based mimicry to disrupt the survivin-Hsp90 interaction, and test its suitability as a novel drug target in cancer.

SIGNIFICANCE

It has long been appreciated that tumor cells are "stressed" cells capable of coping with unfavorable environments via a generalized upregulation of their stress response machinery. This is largely centered on the expression and function of the molecular chaperone Hsp90, which has provided an attractive target for therapeutic intervention in cancer. Here, we report the structure-based design and characterization of shepherdin, a novel peptidomimetic antagonist of the complex between Hsp90 and survivin, another key regulator of tumor cell viability. For its potent and broad antitumor activity, selectivity of action in tumor cells versus normal tissues, and inhibition of tumor growth in vivo without toxicity, shepherdin may offer a promising approach for rational cancer therapy.

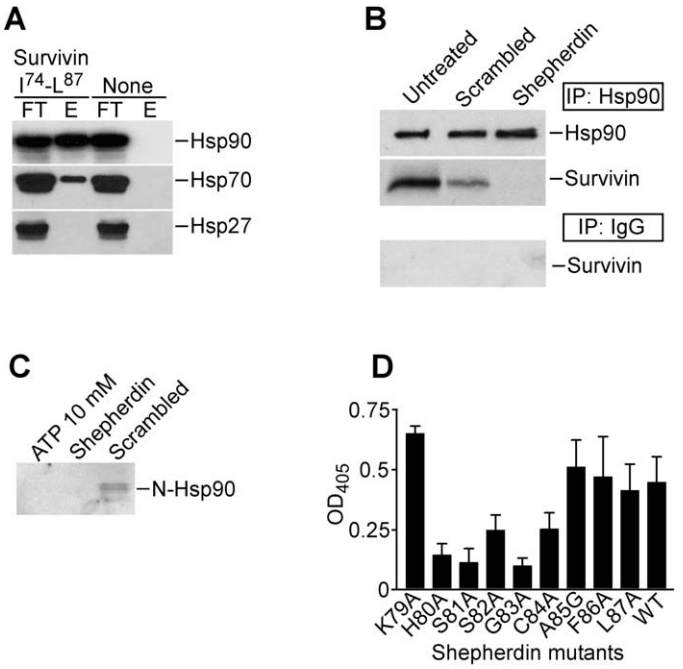

Figure 1. Identification of shepherdin

A: Affinity chromatography. S100 Raji cell extracts were fractionated over control resin or immobilized survivin peptide I74–L87. Flow-through (FT) or eluted (E) material was analyzed by Western blotting.

B: Inhibition of survivin-Hsp90 interaction. Aliquots of rabbit reticulocyte extracts were left untreated or incubated with shepherdin or scrambled peptide, mixed with recombinant survivin, and immunoprecipitated with control IgG or an antibody to Hsp90. The immune complexes were analyzed by Western blotting.

C: Peptide competition of Hsp90-ATP binding. Recombinant Hsp90 N domain was mixed with soluble ATP, shepherdin, or scrambled peptide and incubated with γ-phosphate-linked ATP-sepharose, and bound material was eluted in 5% SDS and analyzed by Western blotting.

D: Peptide mutagenesis. Wild-type or mutant shepherdin peptides were immobilized on plastic microtiter plates and Hsp90 binding was detected by ELISA. Data are the mean ± SD of two independent experiments. WT, wild-type shepherdin.

Results

Identification of shepherdin

Using synthetic peptidyl mimicry, we recently identified a survivin sequence K79–K90, which blocks the interaction between survivin and Hsp90, in vitro (Fortugno et al., 2003). By surface plasmon resonance, the survivin K79–K90 peptide bound Hsp90 with high affinity (K_D ± SEM = 8.38 x 10^{-8} ± 3.5^{-9} M) at increasing ligand concentrations (0.1–10 μM). Conversely, a mutant C84→A peptide (see below) did not bind Hsp90, and exhibited a 10-fold increased off-rate as compared with the wild-type sequence, as shown by surface plasmon resonance. To narrow the minimal interacting region in K79–K90, we tested variant peptides, and found that the sequence I74–L87 retained the ability to bind Hsp90 in vivo with its associated chaperone Hsp70, but not Hsp27, by affinity chromatography of B lymphoma Raji cell extracts (Figure 1A). Therefore, the minimal survivin sequence K79–L87 was named shepherdin for its binding to the "shepherding" chaperone Hsp90. To test whether shepherdin disrupted the survivin-Hsp90 complex in a cellular context, we reconstituted this interaction in reticulocyte extracts, which have been used before to assemble functional Hsp90 complexes (Morishima et al., 2000). Recombinant survivin added to untreated reticulocyte extracts formed a complex with endogenous Hsp90, as detected by coimmunoprecipitation and Western blotting (Figure 1B). In contrast, a control IgG did not immunoprecipitate survivin from reticulocyte extracts (Figure 1B). Preincubation of reticulocyte extracts with shepherdin completely inhibited the association of recombinant survivin with Hsp90, whereas a scrambled peptide had minimal effect (Figure 1B). Next, we asked whether shepherdin interfered with ATP binding to Hsp90 (Marcu et al., 2000). Addition of a scrambled peptide to recombinant N-domain of Hsp90 (residues 1–272) did not affect binding to ATP-sepharose, as shown by affinity chromatography (Figure 1C). In contrast, shepherdin blocked the interaction between N-Hsp90 and immobilized ATP, which was also fully competed out by addition of soluble ATP (Figure 1C). To map the requisites of shepherdin binding to Hsp90, we generated mutant peptides with single amino acid substitutions. Mutagenesis of H80, S81, S82, G83, and C84 abolished shepherdin binding to Hsp90, whereas substitution of K79, A85, F86, or L87 had no effect (Figure 1D). In the survivin crystal structure, amino acids H80–G83 form a flexible loop connecting the fourth and fifth α helices of the baculovirus IAP repeat, and H80 contributes to a surface-exposed "basic patch" (Verdecia et al., 2000).

Structural analysis of shepherdin

Several shepherdin variants were synthesized for further experiments, including a retro-inverso peptidomimetic analog designated shepherdin-RV (inverse sequence L79–K87, all D amino acids). The structures of shepherdin and shepherdin-RV were studied in solution by long time scale molecular dynamics (MD) simulations in explicit water solvent (Supplemental Data and Supplemental Table S1). Analysis of the trajectories predicts that both shepherdin and shepherdin-RV have a dominant configuration characterized by a turn involving S82–G83 in shepherdin and G83–S84 in shepherdin-RV, and overall β-hairpin geometry (Figure 2A). The most populated conformation of shepherdin-RV shows a higher degree of compactness, with the aromatic ring of F80 packing on the turn region (Figure 2A). The representative β-hairpin conformations of shepherdins were subjected to multiple docking experiments on Hsp90 using the AutoDock program package (Morris et al., 1998). In all cases, the peptides were predicted to dock into the ATP binding site of Hsp90 (Figures 2B and 2C). The geometry of the final complex is highly correlated with that of the complex between Hsp90 and GA (Stebbins et al., 1997), with the turn region of the peptides closely tracing the ansa ring backbone of GA (Figures 2D and 2E). Shepherdin and shepherdin-RV make 13 and 18 predicted hydrogen bonds with the ATP pocket of Hsp90, respectively, involving the side chains of H80, S81, S82, the carbonyl group of G83, and the side chains of K87 and C82 (shepherdin-RV). Except for D93, the complementary residues of Hsp90 predicted to make contact with shepherdin and/or shepherdin-RV largely overlap with amino acids implicated in GA binding (Stebbins et al., 1997), including S113, which has been recently shown to contribute to stepwise accessibility of the ATP pocket of Hsp90 to GA (Lee et al., 2004). Shepherdin and shepherdin-RV are predicted to assume more extended conformations than GA in the Hsp90 pocket

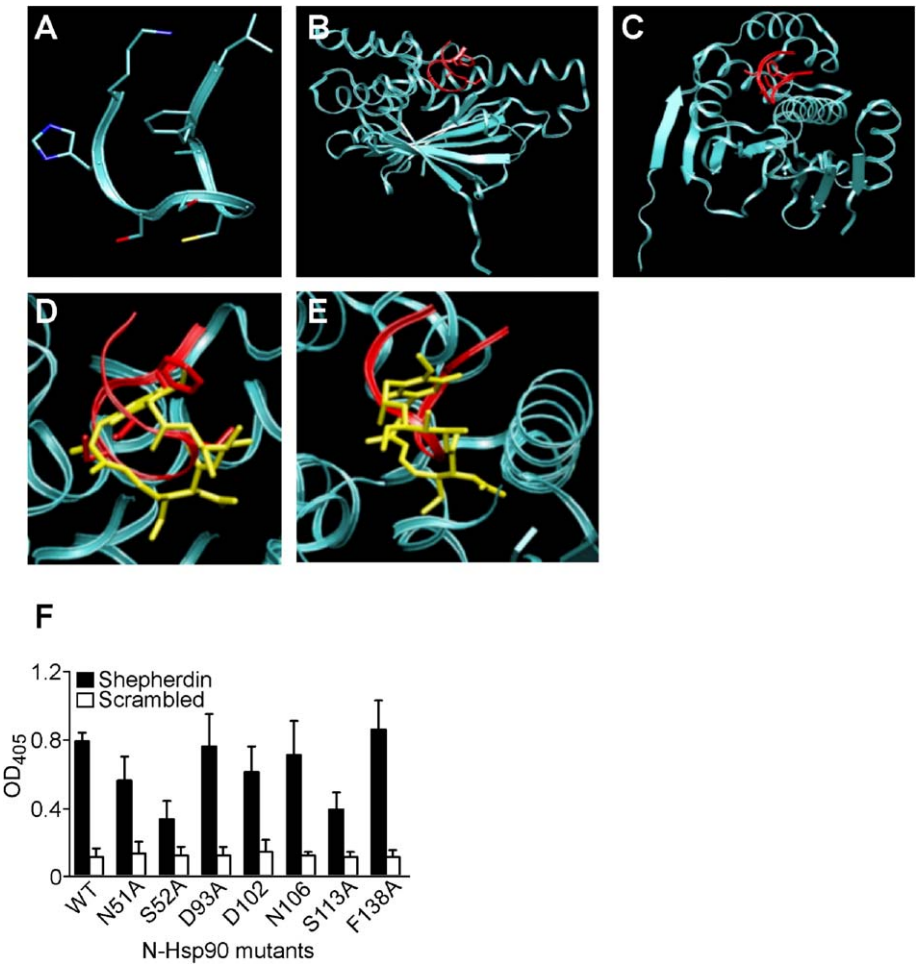

Figure 2. Structural analysis of shepherdin

A: Predictive representative structure of the most populated conformational cluster of shepherdin-RV as calculated from statistical analysis of MD trajectories.

B and C: Two orthogonal views of the dominant structure of shepherdin-RV (ribbon) as obtained by MD simulations are shown overlaid onto the crystal structure of Hsp90.

D and E: Two orthogonal views of shepherdin-RV (red ribbon) in complex with Hsp90 as obtained by docking simulations. The peptide is overlaid onto the crystal structure of GA (yellow) in complex with Hsp90.

F: Hsp90 mutagenesis. The indicated mutants of the N domain of Hsp90 were tested for binding to shepherdin or scrambled peptide. Data are the mean ± SEM of three independent experiments. WT, wild-type N-Hsp90.

(Figures 2D and 2E), and bury a solvent accessible surface of 498 and 546 Å^2, respectively, as opposed to 402 Å^2 buried by GA.

To check these structural predictions, and validate experimentally that shepherdin engaged Hsp90 differently from GA, we introduced targeted mutations in the ATP pocket of Hsp90, and tested their effect on shepherdin binding. Individual substitution of N51, S52, D102, or S113 in the N domain of Hsp90 reduced binding to shepherdin by 20%–60%, whereas mutagenesis of "GA-specific" D93 had no effect, and a scrambled peptide did not bind wild-type or mutant Hsp90 (Figure 2F).

Molecular requirements of shepherdin-Hsp90 recognition

We next tested the interaction of shepherdin with individual domains of Hsp90, and we first analyzed the middle domain (M) for its role in client protein loading (Meyer et al., 2003). Blind docking of shepherdin-RV to the three-dimensional structure of the Hsp90 M domain did not reveal an organized binding pocket, as shown by MD simulations (Figures 3A and 3B). As compared with the extensive network of stabilizing contacts observed for the N domain (Figures 2B–2E), shepherdin-RV docked only to superficial regions of the M domain, mainly through H bonding and electrostatic interactions (Figures 3A and 3B), and buried a considerably smaller surface area (410 Å^2). Next, we compared the direct binding of shepherdin to recombinant N or C domain of Hsp90. Shepherdin associated with the N domain Hsp90 in a concentration-dependent and saturable manner (Figure 3C). In contrast, no specific binding of shepherdin to the C domain of Hsp90 was demonstrated, as compared with scrambled peptide (Figure 3C).

Intracellular delivery of shepherdin induces tumor cell death

Cell-permeable variants of shepherdin were generated by fusing the peptide N termini to either helix III of the *Antennapedia* homeodomain protein (shepherdin^{Atp}) (Kabouridis, 2003) or the HIV-Tat sequence (shepherdin^{Tat}). Both cell-permeable shepherdin variants as well as their control scrambled sequences rapidly (<1 hr) accumulated inside 100% of cervical carcinoma HeLa cells (Figure 4A), and showed identical efficiency of intracellular penetration in single cell fluorescence analysis (Figure 4B). In contrast, shepherdin or a scrambled peptide lacking cell penetrating sequences did not accumulate intracellularly, as shown by fluorescence microscopy (Figure 4A). Comparable confluency of the various cell cultures used in these studies was confirmed by light microscopy (not shown). The IC_{50} of intracellular penetration for shepherdin^{Atp} was 50–75 μM, and 25–30 μM for shepherdin^{Tat}, with the extent of intracellular ac-

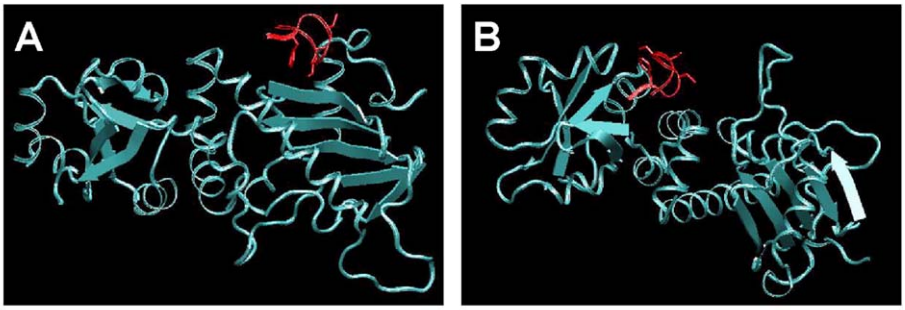

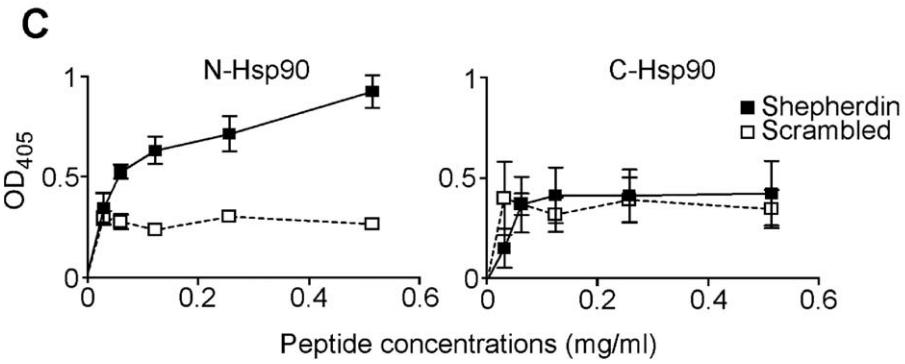

Figure 3. Specificity of shepherdin-Hsp90 interaction

A and B: Two orthogonal views of shepherdin (red) in association with the M domain of Hsp90 obtained by MD docking simulations.

C: Domain-specific interactions. Increasing concentrations of shepherdin or scrambled peptide were immobilized on microtiter wells and incubated with recombinant Hsp90 N or C domain, and protein binding was detected with domain-specific antibodies by ELISA. Data are the mean ± SEM of four independent experiments.

cumulation decreasing sharply at lower peptide concentrations (not shown). Next, we looked at the effect of intracellular delivery of shepherdin, and for all subsequent studies shepherdin^{Atp} was used unless otherwise specified. Treatment of HeLa cells with increasing concentrations of shepherdin resulted in catastrophic loss of cell viability, with the entire cell population exhibiting hypodiploid DNA content, as shown by propidium iodide staining and flow cytometry (Figure 4C). In contrast, a cell-permeable scrambled peptide, or shepherdin peptides without cell penetrating sequences, were without effect (Figure 4C and not shown). In clonogenic assays, cell-permeable shepherdin, but not a scrambled peptide, completely abolished colony formation in soft agar (not shown). To identify the mechanism(s) by which shepherdin killed tumor cells, we examined activation of nonapoptotic and apoptotic cell death pathways. Treatment of HeLa cells with shepherdin^{Atp} or shepherdin^{Tat} resulted in rapid loss of plasma membrane integrity, with the entire cell population becoming Trypan blue-positive by 3–6 hr after peptide addition (Figure 4D). Within the same time frame, shepherdin also induced activation of mitochondrial apoptosis, with release of mitochondrial cytochrome c in the cytosol (Figure 4E). This was accompanied by typical hallmarks of apoptosis, including appearance of annexin V-labeled cells, and expression of caspase activity, as shown by multiparametric flow cytometry (Figure 4F). Preincubation of HeLa cells with a caspase inhibitor, ZVAD-fmk (20 μM), only partially attenuated cell death induced by shepherdin (64.6 ± 10% cell death versus 82.6 ± 4.4% at 125 μM shepherdin, n = 3). Identical results were obtained with cell-permeable shepherdin-RV, which also induced loss of plasma membrane integrity and caspase activation in tumor cells (not shown). Conversely, intracellular accumulation of cell-permeable native or retro-inverso scrambled peptides had no effect on tumor cell viability (Figures 4C–4F and not shown).

Shepherdin inhibits Hsp90 chaperone function

A potential model to explain these findings is that shepherdin engagement of the ATP pocket of Hsp90 (Figures 2B–2F) destabilizes its client proteins, resulting in the acute breakdown of multiple cell survival pathways (Isaacs et al., 2003), including survivin (Fortugno et al., 2003). To test this prediction, we examined the levels of Hsp90 client proteins after intracellular loading of shepherdin or scrambled peptide. Prostate carcinoma PC3 cells treated with shepherdin exhibited loss of multiple Hsp90 client proteins, including survivin, Akt, CDK-4, and CDK-6, as shown by Western blotting (Figure 5A and not shown). In contrast, shepherdin did not affect the levels of Hsp90, Hsp70, or PCNA, and a cell-permeable scrambled peptide did not modulate chaperone or client protein expression (Figure 5A). We also tested the effect of shepherdin on telomerase activity, which requires Hsp90 (Holt et al., 1999). TRAP analysis of Hsp90 immunoprecipitates from PC3 cells revealed that shepherdin treatment almost completely abrogated the enzyme's catalytic activity, as compared with untreated or scrambled peptide-treated cells (Figure 5B). Because of the structural and functional similarities between shepherdin and small molecule Hsp90 antagonist(s), e.g., GA, we compared the antitumor efficacy of shepherdin with that of 17-AAG, a derivative of GA currently in the clinic (Sausville et al., 2003). A 5 hr shepherdin treatment of various tumor cell lines resulted in dose-dependent and complete cell killing (Figure 5C). In contrast, 17-AAG had no effect on tumor cell viability within this time frame (Figure 5C). With a prolonged incubation up to 24 hr, the highest concentration of 17-AAG tested (10 μM)

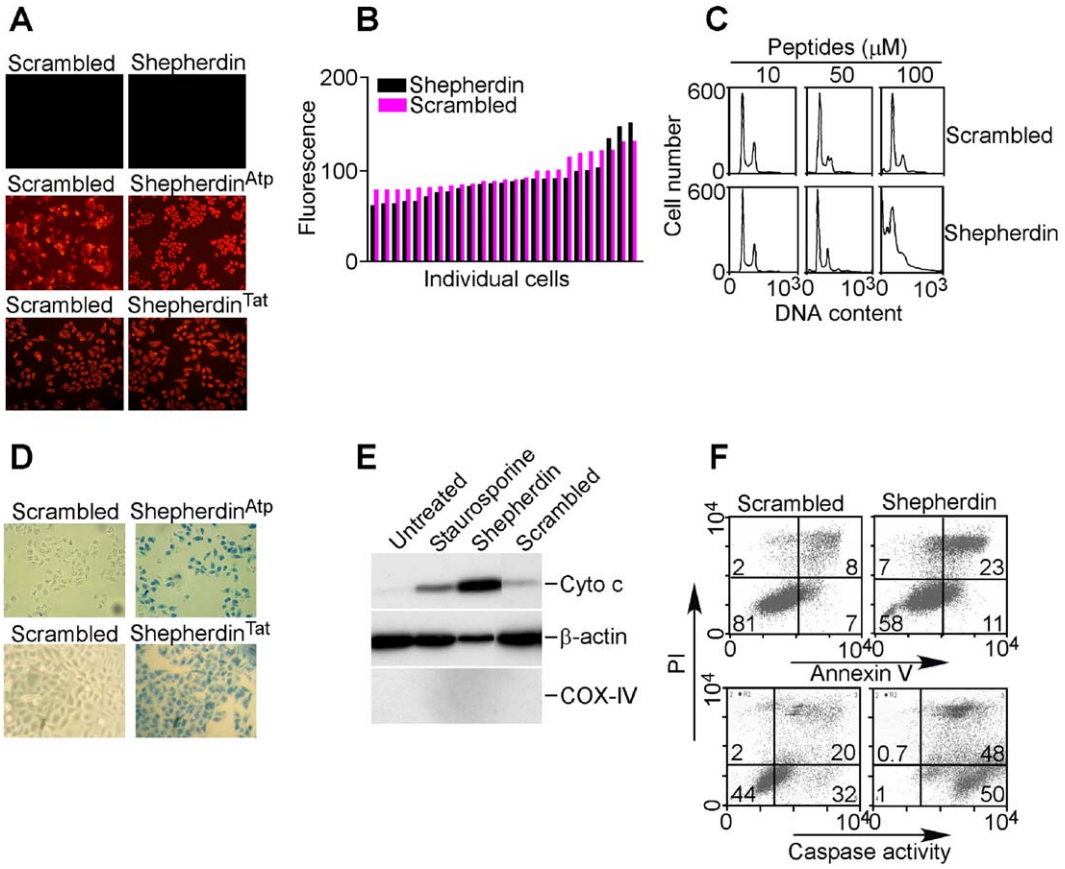

Figure 4. Shepherdin-mediated cell killing

A: Intracellular penetration. HeLa cells were incubated with biotin-conjugated shepherdin (150 μM), cell-permeable shepherdin^{Atp} (150 μM), cell-permeable shepherdin^{Tat} (50 μM), or their respective scrambled peptides at comparable concentrations, labeled with PE-streptavidin, and analyzed by fluorescence microscopy.

B: Single cell analysis. Twenty-five randomly selected cells were analyzed for fluorescence intensity after incubation with shepherdin^{Atp} or scrambled peptide.

C: DNA content analysis. HeLa cells were treated with shepherdin^{Atp} or scrambled peptide, harvested after 18 hr, and analyzed for DNA content by PI staining and flow cytometry.

D: Loss of plasma membrane integrity. HeLa cells were incubated with shepherdin^{Atp} (150 μM), shepherdin^{Tat} (50 μM), or cell-permeable scrambled peptides at identical concentrations, stained for Trypan blue exclusion after 4 hr, and analyzed by light microscopy.

E: Cytochrome c release. Cytosolic extracts isolated from HeLa cells treated with shepherdin^{Atp} or scrambled peptide (150 μM) for 3 hr were analyzed by Western blotting. COX-IV was used as a mitochondrial marker. Staurosporine (1 μM for 16 hr) was used as a control for an apoptotic stimulus.

F: Induction of apoptosis. Cells incubated with shepherdin^{Atp} or scrambled peptide (150 μM) were analyzed after 5 hr by dual-color flow cytometry for Annexin V labeling (HeLa cells, upper panel), or after 12 hr for caspase activity by DEVDase activity (MCF-7 cells, lower panel) in the green channel, and PI staining in the red channel. The percentage of cells in each quadrant is indicated.

produced ~50% cell death (Figure 5C), thus confirming its antitumor activity (Basso et al., 2002).

Requirements of shepherdin-induced tumor cell killing

Tumors with low proliferative index that have lost the p53 tumor suppressor gene, or that upregulate antiapoptotic mechanisms, notably Bcl-2, are likely to become resistant to conventional anticancer therapy (Johnstone et al., 2002), and to evade checkpoint-based "targeted" therapy (Vassilev et al., 2004). Therefore, it was of interest to test whether these conditions affected shepherdin-mediated antitumor activity. Treatment of a panel of tumor cell lines with shepherdin resulted in comparable levels of cell killing whether cells were actively proliferating or made quiescent by prior serum starvation (Figure 6A). Secondly, shepherdin was equally effective at inducing caspase-dependent apoptosis and loss of plasma membrane integrity in p53$^{+/+}$ or p53$^{-/-}$ HCT116 cells (Figure 6B). Lastly, overexpression of Bcl-2 in HeLa cells using a replication-defective adenovirus effectively counteracted apoptosis induced by staurosporine, but did not reduce shepherdin-mediated cell killing (Figure 6C). In all experiments, a cell permeable scrambled peptide was without effect (Figures 6A–6C).

Selectivity of shepherdin antitumor activity

One of the pivotal objectives of "targeted" cancer therapy is to selectively eliminate tumor cells while sparing normal tissues. Therefore, we asked whether shepherdin was a selective anticancer agent, discriminating between normal and tumor cells. When added to prostate carcinoma (PC3, DU145) or HeLa cells, shepherdin caused concentration-dependent and complete loss of cell viability (Figure 7A), consistent with the data presented above. In contrast, identical concentrations of shep-

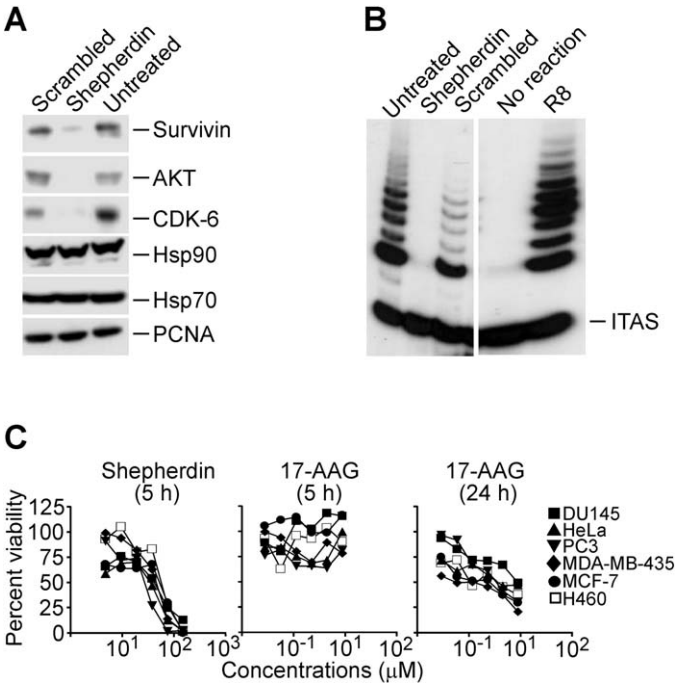

Figure 5. Shepherdin inhibits Hsp90 chaperone function

A: Loss of Hsp90 client proteins. PC3 cells were left untreated or incubated with shepherdin^{ATP} or scrambled peptide (100 μM) for 16 hr and analyzed by Western blotting.

B: Telomerase activity. Hsp90 was immunoprecipitated from peptide-treated PC3 cells and telomerase activity was determined by TRAP assay. R8, external quantitative standard; ITAS, internal amplification standard.

C: Comparison with 17-AAG. The indicated tumor cell lines were treated with shepherdin^{ATP} or 17-AAG and analyzed for cell viability after 5 or 24 hr by MTT.

herdin did not reduce the viability of normal human fibroblasts of three different tissue origins (Figure 7A), and a cell-permeable scrambled peptide had no effect on normal or tumor cells (Figure 7A). Similarly, shepherdin did not reduce the viability of nontransformed mouse embryonic fibroblasts (MEF), whereas it efficiently killed JC mouse mammary carcinoma cells (Figure 7B). Because one of the most serious complications of conventional cancer therapy is the ablation of bone marrow functions, and survivin has been reported to play a role in progenitor cell differentiation (Fukuda et al., 2004), we isolated human CD34$^+$ hematopoietic progenitor cells, and tested the effect of shepherdin on their colony-forming ability. Treatment of purified CD34$^+$ progenitor cells with concentrations of shepherdin sufficient to ablate tumor cell viability (see above) did not significantly reduce colony formation along the erythroid or myeloid lineage, as compared with scrambled peptide-treated cultures (Figure 7C).

Hsp90 has been reported to bind ATP pocket inhibitors, i.e., 17-AAG, with a ~100-fold higher affinity in tumor cells as opposed to normal tissues, and this high-affinity conformation may enhance the tumor selectivity of Hsp90 antagonists (Kamal et al., 2003). To test whether shepherdin also differentially bound Hsp90 from normal or tumor cells, we carried out affinity chromatography experiments. Fractionation of B lymphoma Raji cell extracts over shepherdin-sepharose resulted in the isolation of Hsp90, and coelution of Hsp70, as shown by Western blotting (Figure 7D), and in agreement with the data presented above (Figure 1A). In contrast, chromatography of normal peripheral blood mononuclear cell (PBMC) extracts over shepherdin-sepharose did not yield immunoreactive bands, indicating that shepherdin has little, if any, affinity for Hsp90 in normal cells, and no independent recognition for Hsp70 (Figure 7D). In addition, silver staining analysis of shepherdin-bound material eluted from Raji cell extracts revealed the presence of only two main bands of ~70 and ~90 kDa, demonstrating that shepherdin specificity in vivo is highly restricted (Figure 7E).

Antitumor activity of shepherdin in vivo

To test the efficacy of shepherdin in human cancer models, we first grew prostate carcinoma PC3 cells as superficial tumors in immunocompromised mice, and started treatment when tumors became palpable (~35–70 mm^3). For these studies, shepherdin-RV was used. Control animals given saline exhibited progressive tumor growth during an 11-day interval (Figure 8A). Conversely, administration of shepherdin-RV (50 mg/kg, i.p., daily) nearly completely ablated tumor growth (Figure 8A). Within 1 hr of injection, shepherdin-RV accumulated in the tumor mass, by fluorescence microscopy, whereas tumors of saline-injected animals had only background fluorescence (Figure 8B). Secondly, we tested shepherdin-RV in a breast cancer xenograft model that employs MCF-7 cells adapted in vivo. Injection of these cells in immunocompromised animals resulted in exponentially growing tumors independently of estrogen supplementation, which was unaffected by saline administration (Figure 8C). Conversely, treatment with shepherdin-RV (50 mg/kg i.p. daily) uniformly inhibited the growth of these more aggressive tumors ($p = 0.01$) throughout a 23-day (Figure 8C) or 11-day treatment regimen (not shown). Blood samples taken at the end of treatment revealed no alterations in cell counts or blood chemistry in shepherdin- versus saline-treated animals (Supplemental Table S2). In addition, histologic examination of lung, spleen, and liver was equally unremarkable in the saline or shepherdin group, and extramedullary hematopoiesis in the spleen red pulp occurred with comparable frequency in control or shepherdin-treated mice (Figure 8D). To test whether shepherdin caused loss of Hsp90 client proteins in the context of the tumor mass in vivo, we analyzed MCF-7 tumors recovered at the end of treatment. Tumors from the saline group exhibited extensive labeling for survivin and Akt in the majority of the tumor cell population, as shown by immunohistochemistry (Figure 8E), in agreement with previous observations (Altieri, 2003; Basso et al., 2002). Conversely, shepherdin treatment resulted in nearly complete loss of Akt levels in tumor cells (Basso et al., 2002), and severely attenuated expression of survivin (Figure 8E). Similar results were obtained by Western blotting analysis of tumor cell extracts, with considerable reduction of survivin and Akt levels after shepherdin treatment, as compared with the saline group (Figure 8F).

Discussion

In this study, we used structure-based rational prediction to identify and characterize shepherdin, a novel anticancer peptidomimetic modeled on the survivin-Hsp90 binding interface (Fortugno et al., 2003). Shepherdin engages the ATP pocket of Hsp90 with unique binding characteristics, destabilizes survivin plus several additional client proteins, and causes mas-

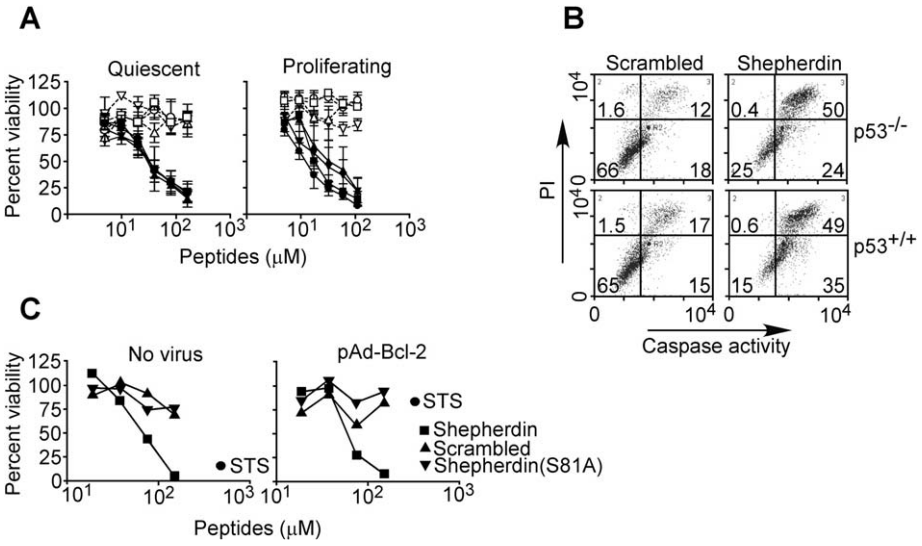

Figure 6. Requirements of shepherdin antitumor activity

A: Independence of cell cycle progression. Tumor cell lines (squares, HeLa; circles, MCF-7; upward triangles, PC3; downward triangles, H-460) were made quiescent by 24 hr serum starvation (quiescent), or maintained in complete growth medium (proliferating), treated with shepherdin^{Atp} (closed symbols) or scrambled peptide (open symbols), and analyzed after 5 hr by MTT. Data are the mean ± SEM of four experiments.

B: p53 independence. $p53^{+/+}$ or $p53^{-/-}$ HCT116 cells were treated with shepherdin^{Atp} or scrambled peptide (150 μM) for 12 hr, and analyzed for caspase activity (DEVDase activity) and loss of plasma membrane integrity by PI staining, by multiparametric flow cytometry. The percentage of cells in each quadrant is indicated.

C: Bcl-2 independence. Untreated (no virus) or HeLa cells transduced with an adenovirus encoding Bcl-2 (pAd-Bcl-2) were incubated with the indicated concentrations of shepherdin^{Atp}, scrambled peptide, or a shepherdin^{Atp} S81A mutant peptide that does not bind Hsp90 (Figure 1C), and analyzed after 12 hr by MTT. Bcl-2 cytoprotection from staurosporine (STS)-induced apoptosis (1 μM) was used as a control.

sive killing of tumor cells by apoptotic and nonapoptotic mechanisms. Shepherdin is selective in its antitumor activity, and does not affect the viability of normal cells or tissues, including human hematopoietic progenitors. When administered in vivo, shepherdin is safe and well tolerated, and inhibits growth of different tumor cell types without systemic or organ toxicity. Taken together, these features may make shepherdin an attractive lead prodrug for "targeted" cancer therapy.

Although initially designed as a high-affinity (K_D ~80 nM) inhibitor of the survivin-Hsp90 interaction, the data presented here suggest that shepherdin may function as a more global antagonist of Hsp90 chaperone activity. This conclusion is based on the structure-function analysis of shepherdin, and in particular its ability to expansively engage the chaperone ATP pocket, compete for the Hsp90-ATP complex, and destabilize multiple Hsp90 client proteins in addition to survivin, in vivo. Because of these features, shepherdin appears ideally suited to interfere with the periodicity of Hsp90 ATPase cycles, by directly preventing ATP binding (Stebbins et al., 1997), and/or by competing with cochaperone recruitment, especially that of $p50^{cdc37}$, which is required for ATPase activity and shares overlapping binding contacts with shepherdin (Roe et al., 2004). In this context, the simultaneous destabilization of survivin levels (Altieri, 2003), combined with the acute collapse of Hsp90 function (Isaacs et al., 2003), would be expected to cause a general breakdown of multiple cell proliferation and cell survival pathways in tumor cells, suitable for therapeutic exploitation (Neckers and Ivy, 2003).

Consistent with this model, a brief exposure of disparate tumor cell lines to cell-permeable variants of shepherdin resulted in massive and complete cell killing via activation of nonapoptotic and apoptotic mechanisms, the latter involving mitochondrial dysfunction, i.e., permeability transition. The concentrations of shepherdin needed to achieve complete tumor cell killing (IC_{50} ~25–75 μM, depending on the cell penetrating sequence), are in line with those of previous studies using cell-permeable carrier sequences (Chen et al., 1999; Sawada et al., 2003), and reflect the efficiency of intracellular penetration rather than the affinity of the mimetic for the target. The ability of shepherdin to trigger both apoptotic and nonapoptotic cell death may explain its broad antitumor activity, which indistinguishably affected tumor cell types of different derivations, regardless of their proliferative condition (Swanton, 2004), p53 status (Vogelstein et al., 2000), or overexpression of potent survival signals, e.g., Bcl-2 (Johnstone et al., 2002), all conditions that typically compromise the efficacy of conventional or "targeted" anticancer therapy (Vassilev et al., 2004). In addition, shepherdin kills tumor cells far more rapidly and more potently than other Hsp90 antagonists currently in the clinic, e.g., 17-AAG (Sausville et al., 2003). As demonstrated by affinity chromatography, this higher antitumor efficacy of shepherdin can not be explained with nonspecific recognition of multiple cellular proteins, and does not involve an independent specificity for Hsp70, a regulator of mitochondrial apoptosis and caspase-independent cell death (Beere, 2004). Conversely, it seems plausible that by virtue of its unique binding interface with Hsp90, shepherdin may disrupt additional, and potentially as yet unrecognized, cell survival functions of the chaperone that are not efficiently compromised by GA or 17-AAG.

When tested as an anticancer agent in tumor models, shepherdin was selective and well-tolerated, sparing normal cells, preserving colony-forming ability of purified human hematopoietic progenitors, and causing no organ or systemic toxicity after prolonged administration in vivo. This desirable selectivity may involve the differential overexpression of survivin and Hsp90 in tumors as opposed to normal tissues (Altieri, 2003; Isaacs et al., 2003), as well as qualitative changes in Hsp90, which exhibits a ~100-fold higher affinity for binding ATP pocket antagonists in tumor versus normal cells. Previously demonstrated for 17-AAG (Kamal et al., 2003), a similar paradigm can be extended to shepherdin, which bound avidly to Hsp90 in lymphoma cells, but not at all in normal human mononuclear cells.

In summary, shepherdin has the molecular features of both

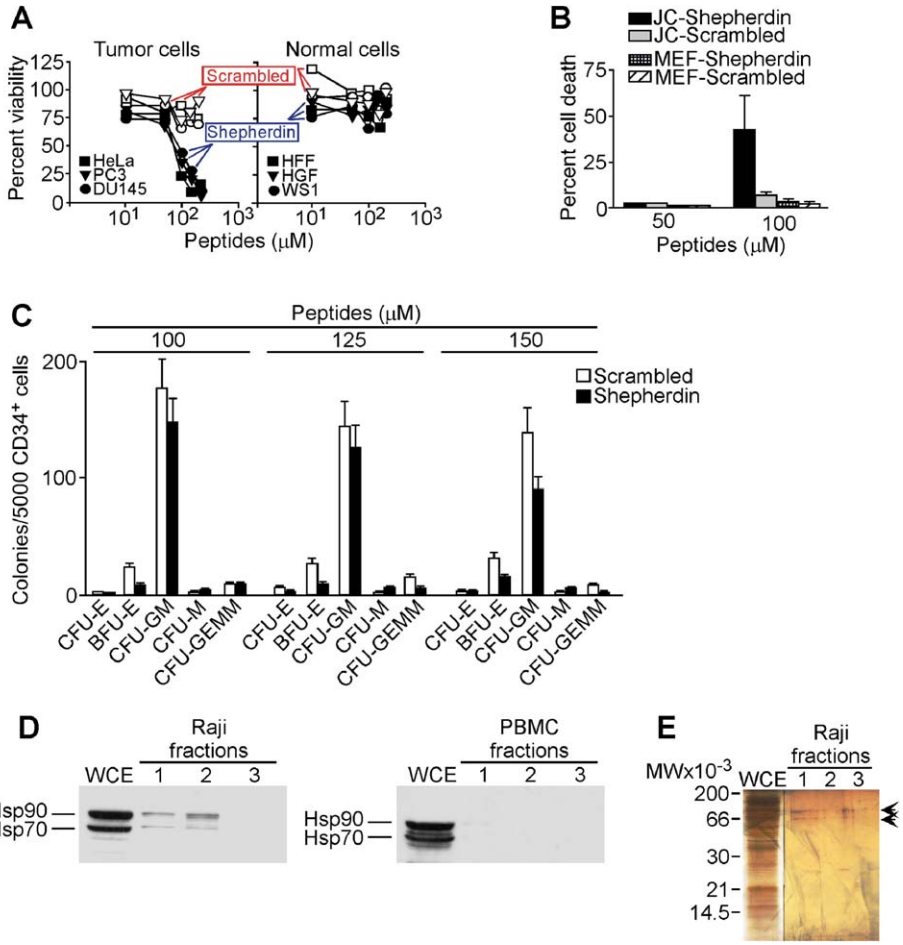

Figure 7. Selectivity of shepherdin-mediated cell killing

A: The indicated tumor or normal cell lines were incubated with shepherdin^{Atp} or scrambled peptide, and analyzed for cell viability after 3 hr by MTT.

B: Analysis of embryonic cells. Mouse embryonic fibroblasts (MEF) or JC mouse mammary carcinoma cells were treated with shepherdin^{Atp} or scrambled peptide, and analyzed by Trypan blue exclusion. Data are the mean ± SEM of three independent experiments.

C: Hematopoietic progenitor colony formation assay. Purified human CD34^{+} hematopoietic progenitor cells were incubated with shepherdin^{Atp} or scrambled peptide for 2.5 hr and plated in semisolid medium with cytokines, and colonies were scored after 10–12 days. CFU-E, colony-forming unit, erythroid; BFU-E, burst-forming unit, erythroid; CFU-GM, colony-forming unit, granulocyte-macrophage; CFU-M, colony-forming unit, macrophage; CFU-GEMM, colony-forming unit, granulocyte, erythroid, macrophage. Data are the mean ± SD of 2 individual replicates.

D: Affinity chromatography. Extracts from B lymphoma Raji cells or freshly isolated normal PBMC were fractionated over shepherdin-sepharose, and eluted material was analyzed by Western blotting. WCE, whole cell extracts.

E: Silver staining. The experimental conditions are the same as in **D**, except that fractions eluted from Raji cell extracts over shepherdin-sepharose were analyzed by silver staining. WCE, whole cell extracts.

an inhibitor of a critical protein-protein interaction in tumor cells, e.g., survivin-Hsp90 (Fortugno et al., 2003), and an enzymatic antagonist of Hsp90 ATPase cycles (Isaacs et al., 2003). Because of these combined features, plus its considerably higher potency compared to other Hsp90 inhibitors, e.g., 17-AAG, shepherdin may provide a potent and selective new anticancer agent in humans, consistent with the use of peptidomimetics in targeted cancer therapy (Guillemard and Saragovi, 2004). In addition, we narrowed the shepherdin binding interface to a short stretch of amino acids between H80 and C84 in the survivin sequence. Previously, mutagenesis of H80 (Muchmore et al., 2000) or C84 (Li et al., 1998) resulted in dominant negative phenotypes with mitotic defects and induction of apoptosis in tumor cells, thus further underscoring their critical roles in survivin function. This small cluster of residues may thus provide a manageable platform for further derivatization of shepherdin, as well as for chemical screenings to identify shepherdin-like small molecules with enhanced, "targeted" anticancer activity in humans.

Experimental procedures

Cells and cell cultures

The following human normal or tumor cell lines were obtained from the American Type Culture Collection (ATCC), and maintained in culture as recommended by the supplier: foreskin fibroblasts HFF, gingival fibroblasts HGF, skin fibroblasts WS-1, prostate adenocarcinoma PC3 and DU145, breast carcinoma MCF-7, B lymphoma Raji, non-small cell lung carcinoma H-460, and cervical carcinoma HeLa. The redesignated melanoma cell line MDA-MB-435LCC6 was kindly provided by Dr. M. Bally (Vancouver, Canada), and p53$^{+/+}$ or p53$^{-/-}$ HCT116 colorectal carcinoma cells were kindly provided by Dr. B. Vogelstein (Baltimore, MD). Mouse embryonic fibroblasts (MEF) and mammary carcinoma JC cells were also obtained from ATCC. Peripheral blood mononuclear cells (PBMC) were isolated from heparinized blood obtained from healthy volunteers after informed consent by Ficoll-Hypaque gradient density centrifugation.

Peptide synthesis and recombinant protein expression

All peptides were synthesized by the W.M. Keck Biotechnology Research Center at Yale University School of Medicine using solid phase tBoc chemistry, followed by reverse-phase high-pressure liquid chromatography, mass spectrometry, and solid phase purification. Peptides were dissolved in water and buffered to pH 7.4. Peptide solutions were prepared fresh every time immediately prior to use, and were not stored. The survivin sequence K79–L87 (KHSSGCAFL, shepherdin) was made cell-permeable by addition of helix III of the cell-penetrating *Antennapedia* homeodomain sequence (underlined) (Kabouridis, 2003), as follows: free/biotin-RQIKIWFQNRRMKWKKKHSSGCAFL-COOH (shepherdin^{Atp}). A corresponding control scrambled peptide was free/biotin-RQIKIWFQNRRMKWKKSKLACFSHG-COOH. A second carrier sequence derived from the HIV Tat protein (Chen et al., 1999) (underlined) and fused at the peptide N termini was also used as follows: biotin-X-YGRKKRRQRRRKHSSGCAFL-CONH$_2$ (shepherdin^{Tat}). A control scrambled peptide using the HIV Tat protein (underlined) was also synthesized as: biotin-X-YGRKKRRQRRRSKLACFSHG-CONH$_2$. X = EAHX, hexanoic acid spacer. Mutant peptides of the shepherdin sequence carrying

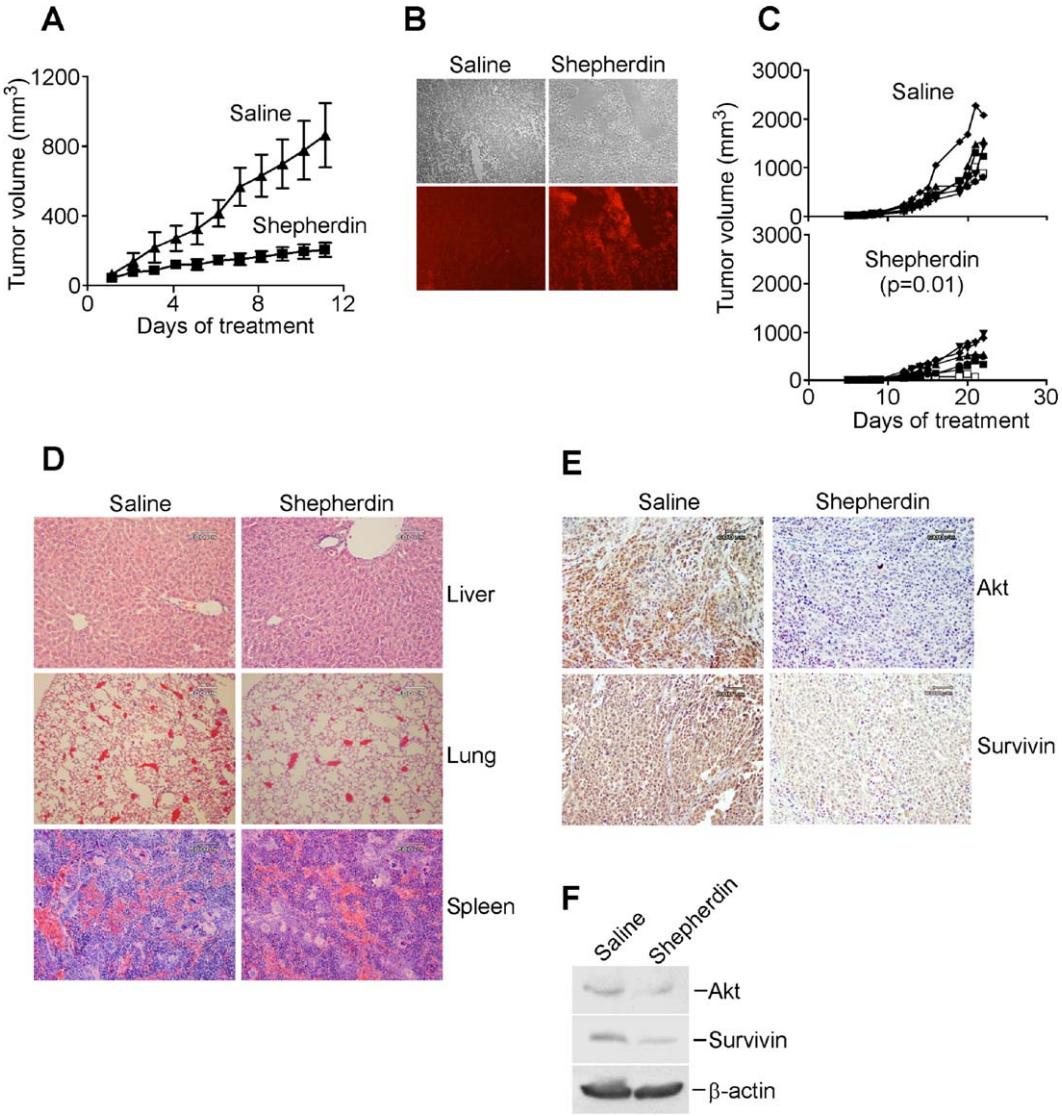

Figure 8. Shepherdin inhibits tumor growth in vivo

A: Kinetics of prostate cancer xenograft growth. SCID/beige mice carrying human PC3 xenograft tumors were treated with daily i.p. injections of saline or cell permeable shepherdin-RV (50 mg/kg) for the indicated time intervals (5/6 animals/group). Tumor volume was measured with a caliper. Data are expressed as mean ± SEM.

B: Intratumor accumulation. Animals were injected i.p. with saline or biotin-shepherdin-RV and sacrificed after 1 hr, and frozen tumor sections were stained with streptavidin-conjugated PE, and analyzed by phase (upper panels) or fluorescence (lower panels) microscopy.

C: Kinetics of breast cancer xenograft growth. SCID/beige mice carrying xenograft tumors from MCF-7 cells adapted in vivo were injected i.p. with saline or cell-permeable shepherdin-RV (50 mg/kg/daily) (6 animals/group) for the indicated time intervals. Each line corresponds to the kinetics of tumor growth of an individual animal.

D: Histology. Formalin-fixed paraffin-embedded tissue sections of liver, spleen or lung from saline- or shepherdin-treated animals were stained by hematoxylin/eosin, and analyzed by light microscopy.

E: Loss of Hsp90 client proteins after shepherdin treatment in vivo. MCF-7 xenografts from saline- or shepherdin-treated animals were harvested at the end of treatment and analyzed with antibodies to survivin or Akt by immunohistochemistry.

F: Western blotting. MCF-7 tumors harvested at the end of saline or shepherdin-RV treatment were analyzed by Western blotting.

single amino acid substitutions at each position were also synthesized. Every residue was mutated to Ala except Ala85, which was changed to Gly. A cell-permeable "retro-inverso" (Pescarolo et al., 2001) shepherdin peptide (shepherdin-RV) fused to the *Antennapedia* sequence was synthesized using Fmoc chemistry and solid phase purification using all D amino acids in the reverse orientation (Herve et al., 1997; Hong et al., 1999), and with Val substituting Ile in the *Antennapedia* sequence (Brugidou et al., 1995) as follows: biotin-X-KKWKMRRNQFWVKVQRLFACGSSHK-$CONH_2$. A control scrambled RV peptide was biotin-X-KKWKMRRNQFWVKVQRGHSFCALKS-$CONH_2$. X = EAHX, hexanoic acid spacer. Individual recombinant Hsp90 domains (N domain, residues 1–272; M domain, residues 273–617; C domain, residues 629–732) cloned in pGex-4T3 (Pharmacia Biotech) and pFLAG-CMV 6c (Sigma) were expressed in BL-21 *E. coli* and purified from the GST frame by overnight thrombin (1 U/ml) cleavage, as described (Fortugno et al., 2003).

Molecular dynamics simulations and docking procedures

The experimental setup for shepherdin computational modeling and docking to Hsp90 is available in the Supplemental Data.

Affinity chromatography and immunoprecipitation

Five mg of survivin peptide I74–L87 carrying an extra cysteine at the N terminus was coupled to 1 ml of Sulfolink coupling gel (Pierce cat n. 20401), as recommended by the manufacturer. To avoid binding to the internal cysteine (C84), this residue was blocked with an Acm group during the synthesis. The block was removed after the binding to the resin by incubation in 10% AcOH, 15 μM mercuric acetate (III), 0.2% β-mercaptoethanol for 6 hr at 22°C. The resin was washed with 16 volumes of 1 M NaCl, and blocked in 10 volumes of 1% BSA overnight at 4°C. 1 x 10^8 Raji cells were collected, washed once in ice-cold TBS, suspended in 4 ml of lysis buffer (25 mM Hepes [pH 7.4], 100 mM KCl, 2 mM EGTA, 1% Triton-X100, 50 mM NaF, 10 mM Na_3VO_4, plus protease inhibitors), and passed trough a 26-gauge needle three times. An S100 fraction was obtained by centrifugation at 100,000 × g for 30 min at 4°C. The cleared lysate (10 mg/ml) was loaded on the survivin peptide resin or an empty resin as control. After washes in lysis buffer, proteins were eluted in 2% SDS, 20 mM Tris (pH 7.5). Samples were separated onto a 12% SDS gel, and analyzed by Western blotting. For peptide competition of Hsp90-ATP interaction (Marcu et al., 2000), three μg of recombinant Hsp90 N domain (1–272) was incubated with 10 mM ATP, shepherdin, or scrambled peptide (150 μM) in 200 μl of molybdate buffer containing 10 mM Tris-HCl (pH 7.5), 5 mM $MgCl_2$, 10 mM $NAMoO_4$, and 0.2% Tween 20 for 2 hr at 4°C under constant agitation. Samples were further incubated with 50 μl of γ-phosphate-linked ATP-sepharose (Boca Scientific) for 2 hr at 4°C and washed, and bound material was eluted in 5% SDS and analyzed by Western blotting. In other experiments, Raji or PBMC cells were lysed in 20 mM Tris, 150 mM NaCl, 1 mM EDTA, 0.5% deoxycholate, 1% Triton X-100 plus protease inhibitors, and extracts (200 μg) were applied to shepherdin-sepharose (5 mg/ml of resin, 0.5 ml) and incubated for 1 hr at 4°C. Bound material was eluted with glycine (pH 2.5) and analyzed by Western blotting or silver staining. A functional survivin-Hsp90 complex was reconstituted in a cellular context using rabbit reticulocyte extracts (Morishima et al., 2000). Aliquots of reticulocyte extracts (35 μl in a total volume of 70 μl) were left untreated or incubated with shepherdin or control peptide (150 μM) for 3 hr at 22°C, mixed with recombinant survivin (1 μg) for 1 hr at 22°C, and immunoprecipitated with control IgG or an antibody to Hsp90. The immune complexes were precipitated with protein G slurry, washed, and probed with antibodies to Hsp90 or survivin by Western blotting.

Protein binding studies

Mutagenesis of the Hsp90 N domain was carried out by PCR, and individual Ala substitutions of N51, S52, D93, D102, N106, S113, and F138 were confirmed by DNA sequencing. Wild-type or mutant Hsp90 constructs were expressed as recombinant fusion proteins in BL-21 *E. coli,* and the GST frame was released by overnight thrombin cleavage (Fortugno et al., 2003). Shepherdin or scrambled peptide (100 μg/ml) was immobilized on plastic microtiter plates, incubated with recombinant Hsp90 (1 μg/ml) or equal concentrations of N domain Hsp90 mutants (5 μg/ml), and further mixed with an antibody to Hsp90 (1 μg/ml). Alternatively, shepherdin or scrambled peptide (0.03–1 mg/ml) was immobilized on plastic microtiter plates, and further incubated with 1 μg/ml of recombinant N- or C-domain of Hsp90 for 1 hr at 37°C. In all experiments, wells were washed 10 times, and binding of the primary antibody was revealed by addition of biotin-conjugated rabbit anti-mouse IgG for 1 hr at 37°C, followed by streptavidine-alkaline phosphatase and determination of absorbance at A_{405} using *p*-nitrophenyl phosphate (Zymed Laboratories, CA) as substrate (Fortugno et al., 2003). An antibody specific for the Hsp90 N domain was purchased from Santa Cruz. A C domain-specific antibody was from BD Transduction.

Cell death assays and analysis of Hsp90 function

Cell viability of various cell lines treated with cell-permeable shepherdin, shepherdin-RV, their control scrambled peptides, or 17-AAG (Calbiochem) was determined by an MTT assay (Sigma, MO) using 200,000 cells/ml (50 μl), or, alternatively, by Trypan blue exclusion. In some experiments, HeLa cells were transduced with an adenovirus encoding Bcl-2 at multiplicity of infection of 50, treated with increasing concentrations of cell-permeable shepherdin^{Atp} or control cell-permeable scrambled peptide, and analyzed by MTT after 12 hr. For determination of apoptosis, peptide-treated cultures were simultaneously analyzed for caspase activity and propidium iodide (PI) staining using CaspaTag (Intergen), or, alternatively, for Annexin V labeling and PI staining, by multiparametric flow cytometry. Mitochondrial release of cytochrome c was assessed in isolated cytosolic extracts of HeLa cells incubated with 150 μM shepherdin^{Atp} or scrambled peptide, by Western blotting. To monitor changes in Hsp90 client protein levels, PC3 cells treated with shepherdin^{Atp} or scrambled peptide (100 μM) were harvested after 16 hr, solubilized in lysis buffer (0.01% NP40, 10 mM Tris [pH 7.5], 50 mM KCl, 5 mM $MgCl_2$, 2 mM DTT, 20% glycerol plus protease inhibitors) plus four pulses on a sonicator (10 s each) at 50 J/Watt-sec, alternated by 30 s intervals on ice, and analyzed by Western blotting. Alternatively, PC3 lysates were immunoprecipitated with a rabbit polyclonal antibody to Hsp90 (Santa Cruz) precoupled to 8 μl of a 50% slurry of protein-G-agarose beads for 1 hr at 4°C. After washes, the immune complexes were analyzed for telomerase activity by telomeric repeat amplification protocol (TRAP) assay using the TRAPeze kit (Intergen, UK). Each reaction product was amplified in the presence of a 36 bp internal TRAP assay standard (ITAS). TSR8 (R8) quantitation standard (which serves as a standard to estimate the amount of product extended by telomerase in a given extract) was included for each set of TRAP assay.

CD34$^+$ hematopoietic stem cell colony formation assay

The experiments were carried out as described previously (Pisarev et al., 2003). Briefly, human CD34$^+$ hematopoietic progenitor cells were isolated from buffy coats of normal healthy volunteers using a magnetic bead separation system (Miltenyi Biotec, Auburn, CA), and incubated with increasing concentrations of shepherdin^{Atp} or scrambled peptide for 2.5 hr at 37°C. CD34$^+$ cells were plated in duplicates into 6-well plates (5,000 cells per well) in 2.5 ml of methylcellulose medium MethoCult GF H4434 (Stem Cell Technologies, Vancouver, Canada), containing cytokines supporting growth of myeloid and erythroid colonies. Colonies were scored on day 10–12.

Xenograft tumor models

All experiments involving animals were approved by an Institutional Animal Care and Use Committee. For in vivo adaptation, 2.5 × 10^6 MCF-7 cells were injected into the flanks of CB-17 SCID/beige mice (Taconics), and grown as solid tumors for 2 weeks. Tumors were excised and minced under sterile conditions, and the derived cell suspension was plated in complete growth media, maintained in a 5% CO_2 humidified incubator at 37°C, and used for further xenograft tumor formation without estrogen supplementation. PC3 or in vivo adapted MCF-7 cells (2.5 × 10^6) were injected into the flanks of CB17 SCID/beige mice, and allowed to form palpable solid tumors for 6–7 days. When tumors reached ~35–70 mm^3 in volume, animals were randomized in 2 groups (4/6 animals/group for PC3 xenografts, and 6 animals/group for in vivo adapted MCF-7 xenografts), and administered saline or shepherdin-RV at 50 mg/kg/daily for 11 consecutive days as i.p. injections (200 μl/injection). In a second MCF-7 experiment, animals were treated with saline or shepherdin (50 mg/kg/daily i.p.) for 23 consecutive days from inoculation. In all experiments, tumor measurements were taken daily with a caliper, and tumor volume was calculated according to the formula 1/2 (length [mm]) × (width [mm])^2.

Toxicity profile

Animals carrying PC3 xenograft tumors were injected i.p. with saline or shepherdin-RV, and sacrificed after 1 hr. The tumors were excised and snap-frozen, and tissue sections were incubated with streptavidin-conjugated PE followed by fluorescence microscopy. Blood samples from animals carrying MCF-7 xenograft tumors and treated with saline or shepherdin-RV were obtained at the end of treatment (day 11, experiment 1). Total cell blood counts were performed on a Heska Veterinary Hematology System. Blood chemistry parameters were determined using the Abaxis VetScan Comprehensive Diagnostic Profile. For histologic analysis, liver, spleen, and lungs were removed from saline- or shepherdin-treated animals carrying MCF-7 xenograft tumors at the end of treatment (day 11, experiment 1). Organs were fixed in formalin and paraffin-embedded, and tissue sections were stained with hematoxylin/eosin and analyzed by light microscopy. Alternatively, MCF-7 breast cancer xenograft tumors were excised at the end of saline or shepherdin treatment (day 23, experiment 2), formalin-fixed, embedded in paraffin, and processed for immunohistochemistry with antibodies against survivin or Akt, according to published protocols (Dohi et al., 2004). In all experiments, a nonbinding IgG was substituted as a primary antibody, and gave no immunoreactivity. In other experiments,

MCF-7 tumors extracted at the end of treatment from the shepherdin or saline group were solubilized, and analyzed by Western blotting with antibodies to survivin or Akt.

Statistical analysis

Data were analyzed using the two-sided unpaired t test on a GraphPad software package for Windows (Prism). A p value of 0.05 was considered as statistically significant.

Supplemental data

Supplemental data for this article can be found at http://www.cancercell.org/cgi/content/full/7/5/457/DC1/.

Acknowledgments

We thank B. Vogelstein for HCT116 cells, M. Bally for MDA-MB-435 cells, T.S. Edgington for discussion, D.S. Garlick for veterinary pathology, and C. Shiffer and C.R. Matthews for reading the manuscript. We also thank J. Crawford and J. Elliott at the W.M. Keck Biotechnology Research Center at Yale University School of Medicine for peptide and peptidomimetic synthesis and characterization. This work was supported by NIH grants HL54131, CA78810, and CA90917, and by grants provided by AIRC (Italian Association for Cancer Research) and the Italian Ministry of Health (grants RF02/171 and RF02/184). M.P. is supported by a fellowship from FIRC.

Received: December 10, 2004
Revised: February 9, 2005
Accepted: March 15, 2005
Published: May 16, 2005

References

Altieri, D.C. (2003). Validating survivin as a cancer therapeutic target. Nat. Rev. Cancer *3*, 46–54.

Basso, A.D., Solit, D.B., Munster, P.N., and Rosen, N. (2002). Ansamycin antibiotics inhibit Akt activation and cyclin D expression in breast cancer cells that overexpress HER2. Oncogene *21*, 1159–1166.

Beere, H.M. (2004). "The stress of dying": The role of heat shock proteins in the regulation of apoptosis. J. Cell Sci. *117*, 2641–2651.

Brugidou, J., Legrand, C., Mery, J., and Rabie, A. (1995). The retro-inverso form of a homeobox-derived short peptide is rapidly internalised by cultured neurones: A new basis for an efficient intracellular delivery system. Biochem. Biophys. Res. Commun. *214*, 685–693.

Chen, Y.N., Sharma, S.K., Ramsey, T.M., Jiang, L., Martin, M.S., Baker, K., Adams, P.D., Bair, K.W., and Kaelin, W.G., Jr. (1999). Selective killing of transformed cells by cyclin/cyclin-dependent kinase 2 antagonists. Proc. Natl. Acad. Sci. USA *96*, 4325–4329.

Dohi, T., Beltrami, E., Wall, N.R., Plescia, J., and Altieri, D.C. (2004). Mitochondrial survivin inhibits apoptosis and promotes tumorigenesis. J. Clin. Invest. *114*, 1117–1127.

Fortugno, P., Beltrami, E., Plescia, J., Fontana, J., Pradhan, D., Marchisio, P.C., Sessa, W.C., and Altieri, D.C. (2003). Regulation of survivin function by Hsp90. Proc. Natl. Acad. Sci. USA *100*, 13791–13796.

Fukuda, S., Mantel, C.R., and Pelus, L.M. (2004). Survivin regulates hematopoietic progenitor cell proliferation through p21WAF1/Cip1-dependent and -independent pathways. Blood *103*, 120–127.

Guillemard, V., and Saragovi, H.U. (2004). Novel approaches for targeted cancer therapy. Curr. Cancer Drug Targets *4*, 313–326.

Herve, M., Maillere, B., Mourier, G., Texier, C., Leroy, S., and Menez, A. (1997). On the immunogenic properties of retro-inverso peptides. Total retro-inversion of T-cell epitopes causes a loss of binding to MHC II molecules. Mol. Immunol. *34*, 157–163.

Holt, S.E., Aisner, D.L., Baur, J., Tesmer, V.M., Dy, M., Ouellette, M., Trager, J.B., Morin, G.B., Toft, D.O., Shay, J.W., et al. (1999). Functional requirement of p23 and Hsp90 in telomerase complexes. Genes Dev. *13*, 817–826.

Hong, S.Y., Oh, J.E., and Lee, K.H. (1999). Effect of D-amino acid substitution on the stability, the secondary structure, and the activity of membrane-active peptide. Biochem. Pharmacol. *58*, 1775–1780.

Isaacs, J.S., Xu, W., and Neckers, L. (2003). Heat shock protein 90 as a molecular target for cancer therapeutics. Cancer Cell *3*, 213–217.

Johnstone, R.W., Ruefli, A.A., and Lowe, S.W. (2002). Apoptosis: A link between cancer genetics and chemotherapy. Cell *108*, 153–164.

Kabouridis, P.S. (2003). Biological applications of protein transduction technology. Trends Biotechnol. *21*, 498–503.

Kamal, A., Thao, L., Sensintaffar, J., Zhang, L., Boehm, M.F., Fritz, L.C., and Burrows, F.J. (2003). A high-affinity conformation of Hsp90 confers tumour selectivity on Hsp90 inhibitors. Nature *425*, 407–410.

Lee, Y.S., Marcu, M.G., and Neckers, L. (2004). Quantum chemical calculations and mutational analysis suggest heat shock protein 90 catalyzes trans-cis isomerization of geldanamycin. Chem. Biol. *11*, 991–998.

Li, F., Ambrosini, G., Chu, E.Y., Plescia, J., Tognin, S., Marchisio, P.C., and Altieri, D.C. (1998). Control of apoptosis and mitotic spindle checkpoint by survivin. Nature *396*, 580–584.

Marcu, M.G., Chadli, A., Bouhouche, I., Catelli, M., and Neckers, L.M. (2000). The heat shock protein 90 antagonist novobiocin interacts with a previously unrecognized ATP-binding domain in the carboxyl terminus of the chaperone. J. Biol. Chem. *275*, 37181–37186.

Meyer, P., Prodromou, C., Hu, B., Vaughan, C., Roe, S.M., Panaretou, B., Piper, P.W., and Pearl, L.H. (2003). Structural and functional analysis of the middle segment of hsp90: Implications for ATP hydrolysis and client protein and cochaperone interactions. Mol. Cell *11*, 647–658.

Morishima, Y., Murphy, P.J., Li, D.P., Sanchez, E.R., and Pratt, W.B. (2000). Stepwise assembly of a glucocorticoid receptor.hsp90 heterocomplex resolves two sequential ATP-dependent events involving first hsp70 and then hsp90 in opening of the steroid binding pocket. J. Biol. Chem. *275*, 18054–18060.

Morris, G.M., Goodsell, D.S., Halliday, R.S., Huey, R., Hart, W.E., Belew, R.K., and Olson, A.J. (1998). Automated docking using a lamarckian genetic algorithm and empirical binding free energy function. J Comp Chem *19*, 1639–1662.

Muchmore, S.W., Chen, J., Jakob, C., Zakula, D., Matayoshi, E.D., Wu, W., Zhang, H., Li, F., Ng, S.C., and Altieri, D.C. (2000). Crystal structure and mutagenic analysis of the inhibitor-of-apoptosis protein survivin. Mol. Cell *6*, 173–182.

Neckers, L., and Ivy, S.P. (2003). Heat shock protein 90. Curr. Opin. Oncol. *15*, 419–424.

O'Dwyer, M.E., and Druker, B.J. (2000). STI571: An inhibitor of the BCR-ABL tyrosine kinase for the treatment of chronic myelogenous leukaemia. Lancet Oncol. *1*, 207–211.

Okada, H., and Mak, T.W. (2004). Pathways of apoptotic and non-apoptotic death in tumour cells. Nat. Rev. Cancer *4*, 592–603.

Paez, J.G., Janne, P.A., Lee, J.C., Tracy, S., Greulich, H., Gabriel, S., Herman, P., Kaye, F.J., Lindeman, N., Boggon, T.J., et al. (2004). EGFR mutations in lung cancer: Correlation with clinical response to gefitinib therapy. Science *304*, 1497–1500.

Pescarolo, M.P., Bagnasco, L., Malacarne, D., Melchiori, A., Valente, P., Millo, E., Bruno, S., Basso, S., and Parodi, S. (2001). A retro-inverso peptide homologous to helix 1 of c-Myc is a potent and specific inhibitor of proliferation in different cellular systems. FASEB J. *15*, 31–33.

Pisarev, V., Yu, B., Salup, R., Sherman, S., Altieri, D.C., and Gabrilovich, D.I. (2003). Full-Length Dominant-Negative Survivin for Cancer Immunotherapy. Clin. Cancer Res. *9*, 6523–6533.

Roe, S.M., Ali, M.M., Meyer, P., Vaughan, C.K., Panaretou, B., Piper, P.W., Prodromou, C., and Pearl, L.H. (2004). The Mechanism of Hsp90 regulation by the protein kinase-specific cochaperone p50(cdc37). Cell *116*, 87–98.

Sausville, E.A., Tomaszewski, J.E., and Ivy, P. (2003). Clinical development of 17-allylamino, 17-demethoxygeldanamycin. Curr. Cancer Drug Targets *3*, 377–383.

Sawada, M., Hayes, P., and Matsuyama, S. (2003). Cytoprotective membrane-permeable peptides designed from the Bax-binding domain of Ku70. Nat. Cell Biol. *5*, 352–357.

Sieber, O.M., Heinimann, K., and Tomlinson, I.P. (2003). Genomic instability–the engine of tumorigenesis? Nat. Rev. Cancer *3*, 701–708.

Stebbins, C.E., Russo, A.A., Schneider, C., Rosen, N., Hartl, F.U., and Pavletich, N.P. (1997). Crystal structure of an Hsp90-geldanamycin complex: Targeting of a protein chaperone by an antitumor agent. Cell *89*, 239–250.

Swanton, C. (2004). Cell-cycle targeted therapies. Lancet Oncol. *5*, 27–36.

Vassilev, L.T., Vu, B.T., Graves, B., Carvajal, D., Podlaski, F., Filipovic, Z., Kong, N., Kammlott, U., Lukacs, C., Klein, C., et al. (2004). In vivo activation of the p53 pathway by small-molecule antagonists of MDM2. Science *303*, 844–848.

Verdecia, M.A., Huang, H., Dutil, E., Kaiser, D.A., Hunter, T., and Noel, J.P. (2000). Structure of the human anti-apoptotic protein survivin reveals a dimeric arrangement. Nat. Struct. Biol. *7*, 602–608.

Vogelstein, B., and Kinzler, K.W. (2004). Cancer genes and the pathways they control. Nat. Med. *10*, 789–799.

Vogelstein, B., Lane, D., and Levine, A.J. (2000). Surfing the p53 network. Nature *408*, 307–310.

Young, J.C., Moarefi, I., and Hartl, F.U. (2001). Hsp90: A specialized but essential protein-folding tool. J. Cell Biol. *154*, 267–273.